

**UNCONSOLIDATED CERES MODEL HAS A WARM CONVECTING ROCKY CORE AND A CONVECTING MUD OCEAN.** B. J. Travis<sup>1</sup>, P. A. Bland<sup>2</sup>, W. C. Feldman<sup>1</sup>, M. V. Sykes<sup>1</sup>, <sup>1</sup>Planetary Science Institute, 1700 E. Ft. Lowell, Suite 106, Tucson, AZ 85719 (btravis@psi.edu); <sup>2</sup>Department of Applied Geology, Curtin University, Perth, WA 6845, Australia.

**Background:** Ceres is an intriguing object. Ceres' low density ( $2077 \text{ kg/m}^3$ ) suggests it may contain large amounts of  $\text{H}_2\text{O}$ . A recent analysis [1] concludes that Ceres must in fact contain a large free water fraction. Kueppers et al. [2] recently reported on water vapor emanating from two regions near Ceres' surface – possibly due to sublimation or to cryovolcanism. Emissions amount to about 6 kg/s from each area. McCord and Sotin's [3] thermal evolution models confirm that radiogenic heating could have melted any water ice present earlier in its history, leading to complete differentiation of Ceres. Observations from the Hubble Space Telescope (HST) and near-IR data confirm that the shape of Ceres is consistent with a differentiated body [4]. The shape and density measurements suggest that Ceres has an ice layer 30–80 km thick overlying a rocky core [3]. Castillo-Rogez and McCord [5] developed more refined thermal models that indicate the rocky core may be further differentiated into hydrated and dehydrated layers. Earth-based spectroscopy has revealed hydrated minerals on Ceres' surface, including brucite, carbonates such as dolomite, iron-rich clays and even magnetite [6, 7].

**Modeling:** Numerical modeling of dynamics in Ceres can provide constraints on its past and present internal states. Ceres appears to have considerable  $\text{H}_2\text{O}$  content. This raises the possibility of aqueous activity in its interior at some point in its history. A recent modeling study of Ceres [5] suggests hydrothermal processes merit further investigation. For Ceres' early history, thermal models and reasonable estimates of the Rayleigh number indicate strong fluid flow should occur. Hydrothermal activity can change the internal state significantly relative to a no-flow state, e.g., by reducing peak temperature, changing ice shell thickness and producing heterogeneous pressure differentials. Further, convective activity can generate numerous upwelling plumes of warmer fluid that can modify topography on the bottom of an ice shell and induce convection in an overlying ice shell, leading to non-uniform heat flux at the surface.

This study employs the MAGHNUM numerical simulator. The MAGHNUM numerical code has been applied to the study of a number of planetary objects, including small asteroids and planetesimals [8]. During their early history, decay of  $^{26}\text{Al}$  and  $^{60}\text{Fe}$  could generate enough heat to thaw the interior of such bodies and drive a period of hydrothermal circulation. Further, MAGHNUM, coupled with the USGS chemistry code PHREEQC [9], was used to model hydration reactions

in planetesimals [10]. Recently Bland et al [11] modified it to simulate evolution of asteroids from frozen unconsolidated mixtures of ice crystals and rock grains through to core formation. Further, Schubert et al [12] and Travis et al [13] used MAGHNUM to model the whole moon history of Enceladus, and Travis et al. [14] did the same for Europa. The equations solved include mass conservation, momentum conservation, energy conservation and solute conservation, with equation of state and constitutive relations.

**Ceres Model:** A preliminary two-dimensional simulation of Ceres covering most of its history has been carried out to discover the kind of internal dynamics that is possible, under the constraints of conservation laws and thermodynamics. Our 2-D model is a continuation of an early-time simulation, starting at CAI + 2 Myr, of the evolution of a frozen mixture of ice and silica grains into a permeable silicate core and a mud ocean under an ice shell [11]. Hydrothermal activity in the rocky permeable core is coupled to flow in an ocean layer and to heat transfer in a developing ice shell.

Applied surface temperature varies from 150 K at the poles to 170 K at the equator. Radius is 476 km, and the over-all density is  $2077 \text{ kg/m}^3$ . Model geometry is spherical (radius, latitude). Our simulation covers evolution of the interior from its early history to near-present. Gravity is a function of depth and surface gravity is  $0.278 \text{ m/s}^2$ . The ice shell evolves over time and location in response to local dynamics. Sub-grid-scale flow dynamics in the ocean layer and the ice shell are parameterized through effective thermal conductivity as function of a local Rayleigh number-Nusselt number relation. The grid mesh used for the simulation has 128 nodes in latitude, and 100 in the radial, with non-uniform spacing radially (larger node spacing in the core region, diminishing to smaller, uniformly spaced nodes in the outermost 200 km). This provides good accuracy in the core, mantle and ice shell. The rocky core is roughly 300 km in radius. Ocean mud density is about  $1870 \text{ kg/m}^3$ .

**Results:** In our model simulation, the internal temperature peaks very early at about  $200 \text{ }^\circ\text{C}$ , from decay of  $^{26}\text{Al}$  and  $^{60}\text{Fe}$ , then drops off by about 150 Myr into the simulation to about  $35 \text{ }^\circ\text{C}$ . At this point, long-term radiogenic heating (from  $^{235}\text{U}$ ,  $^{238}\text{U}$ ,  $^{232}\text{Th}$ ,  $^{40}\text{K}$ ) almost balances heat loss through the surface, and the internal peak temperature drops very slowly. Hydrothermal circulation in the rocky core and ocean sets up by 100 Myr after start-up. Internal heating in the rocky core

plus cold, sinking plumes from the surface drive the convective circulation. Initially, the flow pattern is dipolar, but transitions to a quadrupole pattern between 200 and 500 Myr. Figure 1 displays the temperature distribution at 0.5 Gyr. The large warm upwellings in the rocky permeable core feed smaller scale convection in the ocean layer. Flow in the ocean layer is more dynamic than in the core. Convection cells in the ocean layer are roughly 100 km wide vs. about 450 km in size in the rocky core. The ice shell is slowly thickening, but is still only about 10 km (above major plumes) to 40 km (poles) thick, at 0.5 Gyr. The four large plumes in the core are unsteady, pulsating over time, driving unsteady smaller scale convection cells in the mud ocean layer. Asymmetry is a result of random initial perturbations and the time-dependent nature of the convection under the assumed conditions.

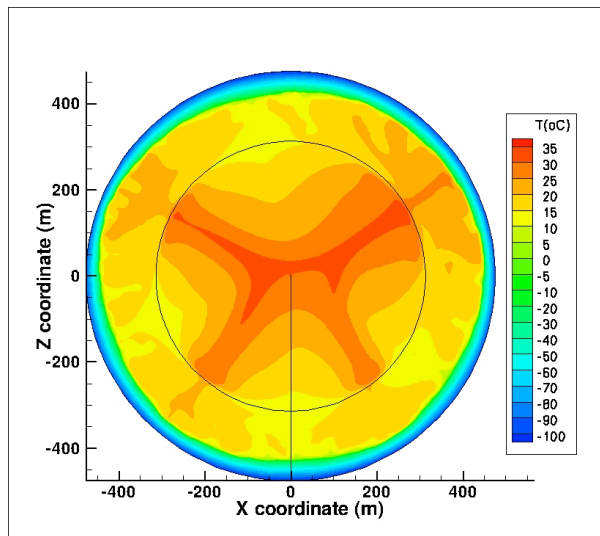


Figure 1 Early time (0.5 Gyr) temperature distribution.

As noted, peak internal temperature slowly decreases, as seen in Figure 2, at a rate of roughly 4-6 °C/Gyr. The small scale fluctuations correspond to pulsations in the large convective plumes.

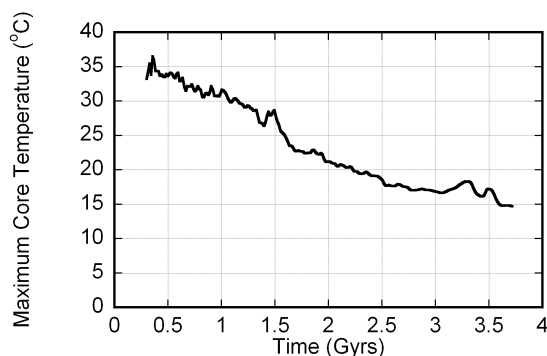


Figure 2 Peak core temperature vs time

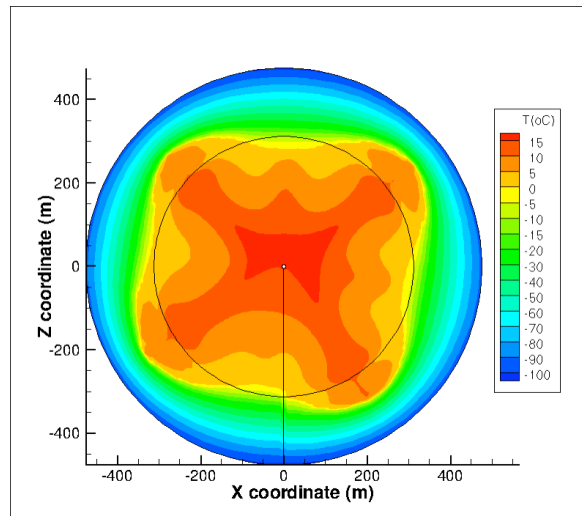


Figure 3 Temperature distribution at 4 Gyr.

In Figure 3, at 4 Gyr into the simulation, heat flow has diminished greatly, to  $\sim 1 \text{ mW/m}^2$ , as long-lived radio-nuclides decay. The mud ice shell thickness is variable, ranging from 75 km above upwellings to  $\sim 125 \text{ km}$  in colder regions. There are four regional seas, about 60-75 km deep, and about 100-200 km wide. The core region is the main locus of hydrothermal activity. The pulsing quadrupole convection in the core continues.

Our simulation suggests that liquid water could still be present and active in the interior of Ceres. Factors not included in the model (e.g., serpentinization, freezing point lowering due to salts in water, pressurization from thickening ice shell) could extend or expand an ocean, and will be explored in future simulations. Assuming that our model approximates Ceres' initial state (melting of an unconsolidated mix of ice, fines, and rocky grains) it appears likely that hydrothermal convection in a mud ocean and wet rocky core is on-going.

**References:** [1] Castillo-Rogez J. C. (2011) *Icarus*, 215, 599. [2] Koppers M. et al. (2014) *Nature* 505, 525. [3] McCord T. B. and Sotin C. (2005) *JGR*, 110, E05009. [4] McCord T. B. et al. (2006) *EOS Trans. AGU*, 87, 105-109. [5] Castillo-Rogez J. C. and McCord T. B. (2010) *Icarus*, 205, 443. [6] Milliken R. E. and Rivkin A. S. (2009) *Nature Geol.*, 2, 258-261. [7] Rivkin A. S. et al. (2011) *Space Sci. Rev.*, 163, 95-116. [8] Travis B. J. and Schubert G. (2005) *EPSL*, 240, 234-250. [9] Parkhurst D. L. and Appelo C. A. J. (1999) *US Dept Interior USGS Water Resources Report 99-4259*. [10] Palguta J., Schubert G., and Travis B. (2010) *EPSL* 296, 235-243. [11] Bland P. A., Travis B. J., Dyl K. A. and Schubert G. (2013) *LPS XLIV*, Abstract #1447. [12] Schubert G. et al. (2007) *Icarus*, 188, 345-355. [13] Travis B. J. and Schubert G. (2015) *Icarus*, 250, 32-42. [14] Travis B. J., Palguta J. and Schubert G. (2012) *Icarus*, 218, 1006-1019.